# Sensitivity-Enhanced Fluidic Glucose Sensor Based on a Microwave Resonator Coupled With an Interferometric System for Noninvasive and Continuous Detection

Chorom Jang, *Graduate Student Member, IEEE*, Jin-Kwan Park, *Graduate Student Member, IEEE*, Hee-Jo Lee, *Member, IEEE*, Gi-Ho Yun, and Jong-Gwan Yook, *Senior Member, IEEE*

***Abstract*—In this paper, a microwave fluidic glucose sensor based on a microwave resonator coupled with an interferometric system is proposed for sensitivity enhancement. The proposed glucose sensor consists of two parts: a sensing part and a sensitivity enhancement part. The former is composed of a rectangular complementary split ring resonator (CSRR), and the latter is composed of a variable attenuator, a variable phase shifter, two hybrid couplers, and an RF power detector. Because the variation in the electrical properties, which is utilized in the microwave detection scheme, with glucose concentration over the possible concentration range in the human body is very small, improvement of the sensitivity is critical for practical use. Thus, the effective sensing area of the rectangular CSRR is determined by considering the electric field distribution. In addition, magnitude and phase conditions for the effective sensitivity enhancement are derived from a mathematical analysis of the proposed interferometric system. In the present experiment, aimed at demonstrating the detection performance as a function of the glucose concentration in the range of 0 mg/dL to 400 mg/dL, the sensitivity is significantly improved by 48 times by applying the derived conditions for effective sensitivity enhancement. Furthermore, the accuracy of the proposed glucose sensor for glucose concentrations at a step of 100 mg/dL is verified by the Clarke error grid. Based on the measurement results, the proposed glucose sensor is demonstrated to be applicable to noninvasive and continuous monitoring in practical environments.**

***Index Terms*—Complementary split ring resonator, glucose sensor, interferometric system, noninvasive detection, real-time monitoring, sensitivity enhancement.**

Manuscript received June 17, 2021; revised August 7, 2021; accepted August 25, 2021. Date of publication September 27, 2021; date of current version December 9, 2021. This work was supported in part by the Basic Science Research Program through the National Research Foundation of Korea (NRF) funded by the Ministry of Education under Grant NRF-2021R1A6A3A13046764. This paper was recommended by Associate Editor Prof. S. Leonhardt. *(Corresponding author: Jong-Gwan Yook.)*

Chorom Jang, Jin-Kwan Park, and Jong-Gwan Yook are with the Department of Electrical & Electronic Engineering, Yonsei University,Seoul, 03722, South Korea (e-mail: chorom@yonsei.ac.kr; paladin91@yonsei.ac.kr; jgyook@yonsei.ac.kr).

Hee-Jo Lee is with the Department of Physics Education, College of Education, Daegu University, Daegu 38453, South Korea (e-mail: hjlee@daegu.ac.kr).

Gi-Ho Yun is with the Department of Information and Communication Engineering, Sungkyul University, Anyang 14097, South Korea (e-mail: ghyun@sungkyul.ac.kr).

Color versions of one or more figures in this article are available at https://doi.org/10.1109/TBCAS.2021.3112744.

Digital Object Identifier 10.1109/TBCAS.2021.3112744

## I. Introduction

DIABETES mellitus, which is a metabolic and chronic disease, is a crucial global health problem due to the difficulty in complete recovery and the surge in the number of patients and deaths. According to the diabetes atlas report of the International Diabetes Federation (IDF), the estimated number of diabetic patients was 463 million people in 2019 and will be 578 million people by 2030 and 700 million people by 2045 [1]. Additionally, the IDF estimated the number of deaths attributable to diabetes in adults from 20 to 79 years old in 2019. Throughout the world, 11.3% of the population dies from diabetes, which is equivalent to one in nine adults aged 20-79 confronting death from diabetes [2]. In particular, diabetic patients with a hyperglycemic state, defined as blood glucose levels exceeding 230 mg/dL [3], have a high risk of mortality because of organ damage such as heart disease, stroke, renal failure, and diabetic foot [4], [5]. Similarly, patients with a hypoglycemic state, defined as blood glucose levels below 70 mg/dL [6], have a relatively high probability of death compared to patients with a hyperglycemic state due to shock and brain damage [7]. For these reasons, to maintain the blood glucose level in the normal range, diabetic patients should monitor their glucose levels several times a day. In general, blood glucose levels are quantified by an invasive method, which involves measurement by pricking a fingertip using a disposable lancet and a test strip of a commercial glucometer. This process is painful, uncomfortable, and time consuming and causes significant economic problems. The IDF estimated that the global diabetes-related health expenditure was USD 760 billion in 2019 and will be USD 825 billion by 2030 and USD 845 billion by 2045 [8]. To improve the quality of life of diabetic patients, the minimally invasive method has gained attention in recent decades [9]–[11]. This method can alleviate pain because of the use of microneedles, but the economic burden of periodically replacing the needles remains. Additionally, a risk of infection even exists due to the small scars caused by the pricking process.

Considering these limitations, an electromagnetic field-based sensing technique utilizing the penetration ability of electromagnetic waves can be an alternative for noninvasive glucose sensing. In general, with changing electrical properties of the

material under test (MUT), the characteristics of microwave devices vary due to the interaction of electromagnetic fields with the MUT. Namely, as the glucose concentration changes, the electrical properties, such as the dielectric constant and loss tangent, are changed [12]. Therefore, the glucose concentration can be detected by using the variation in the characteristics of microwave devices. Microwave-based glucose detection based on this sensing mechanism does not cause any pain or risk of infection in diabetic patients because the skin tissue is not physically pierced [13]. In addition, since microwave devices do not require any enzymes or replacement of sensing components, they are reusable and allow continuous glucose monitoring (CGM) [14]–[16]. Because of these advantages, microwave-based noninvasive glucose sensors have been reported in recent decades [17]–[23]. However, these sensors are bulky and require a considerable volume of blood, posing a number of problems in practical use. On the other hand, glucose sensors based on a microwave planar resonator type have been proposed [24]–[32]. In particular, near-field resonators can focus the electromagnetic field over a short distance at the resonant frequency. Thus, the glucose concentration can be detected by locating the glucose solution in the sensing area of the resonator, where the electromagnetic field is highly concentrated. Despite significant developments in noninvasive glucose detection methodologies, the challenge of improving the sensitivity remains because the variation in the electrical properties with glucose concentration over the reasonable blood glucose range of a human body is very subtle [33]. Additionally, electromagnetic waves rapidly decay in the skin and muscle layers due to the high water content [34]. Therefore, sensitivity enhancement of the microwave-based glucose sensor is necessary for practical use. To overcome the limited sensitivity due to lossy environments such as water-based samples, numerous studies involving various methodologies, such as phase cancellation with a feedback loop [35], inherent high sensitivity [36], metamaterial coupling [37], loss-compensated active resonators [38]–[40], and utilization of the 7th intermodulation product [41], have been published. These methods perform detection mainly by frequency variation, that require a frequency sweep and vector network analyzer (VNA) calibration.

In this paper, a novel noninvasive and continuous glucose sensor using the level variation of the transmission coefficient as a sensing parameter based on a microwave resonator coupled with an interferometric system for sensitivity enhancement is proposed and validated. First, the principle of the proposed sensor system for sensitivity enhancement is mathematically analyzed. Then, the design of the microwave resonator and the interferometric system is presented. Finally, the performance of the proposed glucose sensor is validated by experimental results comparing direct detection and enhanced sensitivity detection.

## II. Principle of the Proposed Sensitivity Enhancement System

In this work, glucose detection using a microwave resonator is realized based on the variation in the transmission coefficient ($S_{21}$) as a function of glucose concentration. In addition, the proposed sensitivity enhancement is implemented by combining the resonator with an additional interferometric circuit. Prior to analyzing the proposed sensor system, the transmission characteristics of the resonator for a glucose concentration, which are the basis of detection, are presented.

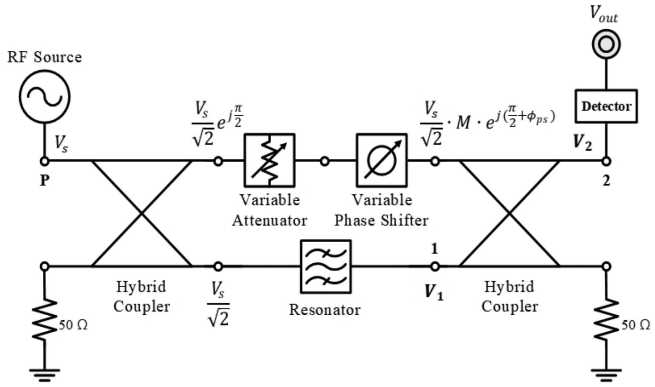


Fig. 1. Schematic of the proposed sensitivity-enhanced glucose sensor.

When a solution with a time-varying glucose concentration is loaded onto the sensing area of the resonator, the magnitude and phase of the transmitted signal are modulated based on the glucose concentration as follows:

$$V_{tr}(t) = V_s \cdot |T_r| \cdot |1 + \tau_g(t)| \cdot e^{j(\angle T_r + \angle \tau_g(t))}, \quad (1)$$

where $V_s$ and $V_{tr}$ represent the input and output signals of the resonator, respectively. $|T_r|$ and $\angle T_r$ are the magnitude and phase of the resonator, and $\tau_g(t)$ and $\angle \tau_g(t)$ are those of the time-varying glucose concentration. With changing glucose concentration, the magnitude and phase variations are very small. In this study, magnitude variation for sensitivity enhancement is considered. Thus, the transmitted signal of the resonator in the case of narrowband modulation can be simplified as follows [42]:

$$V_{tr}(t) = V_s \cdot |T_r| \cdot |1 + \tau_g(t)| \cdot e^{j(\angle T_r)}. \quad (2)$$

Then, the transfer function of the resonator can be expressed as follows:

$$h_r(t) = |T_r| \cdot |1 + \tau_g(t)| \cdot e^{j(\angle T_r)}. \quad (3)$$

As mentioned above, similar to the case of the resonator, the transfer function of the proposed sensitivity enhancement system is analyzed. A schematic of the proposed system is shown in Fig. 1. The proposed glucose sensor for enhancing the sensitivity consists of a resonator for glucose concentration detection, a variable attenuator and a variable phase shifter for modeling the resonance characteristics of the resonator, two hybrid couplers to obtain out-of-phase signals, and an RF power detector for simple and inexpensive measurement. Here, the magnitude of the variable attenuator is $M$, while the phase of the variable phase shifter is $\phi_{ps}$. When source voltage $V_s$ is applied to the proposed system, the output voltage ($V_1$) of the resonator with a time-varying glucose concentration can be expressed as follows:

$$V_1(t) = \frac{V_s}{\sqrt{2}} |T_r| \cdot |1 + \tau_g(t)| \cdot e^{j(\angle T_r)}. \quad (4)$$

The input of the RF power detector ($V_2$) is the sum of $V_1$ and the output voltage of the modeling part with a $90^\circ$ phase difference, which can be modeled as follows:

$$V_2(t) = \frac{V_s}{2}\left[|T_r|\cdot|1+\tau_g(t)|\cdot e^{j(\angle T_r)} + M\cdot e^{j(\pi+\phi_{ps})}\right]. \tag{5}$$

Therefore, the transfer function of the proposed sensor system can be derived as:

$$h_p(t) = \frac{1}{2}\left[|T_r|\cdot|1+\tau_g(t)|\cdot e^{j(\angle T_r)} + M\cdot e^{j(\pi+\phi_{ps})}\right]. \tag{6}$$

The RF power detector is a device that converts RF power to DC voltage, with the output being linearly proportional to the input. The output voltage of the RF power detector can be modeled when operating in the linear region as follows:

$$V_{out} = D(V_i) = k\cdot 20\cdot\log_{10}(V_i) + V_c, \tag{7}$$

where $k$ and $V_i$ are an arbitrary constant and the input voltage of the RF power detector, respectively. $V_c$ is a constant corresponding to the minimum detectable RF power input. Because the sensitivity of the detector is defined as the slope of the output to the input, the sensitivities according to small signal analysis of a microwave resonator ($S_r$) and the proposed system ($S_p$) are as follows [43]:

$$\begin{aligned} S_r &\triangleq \frac{\partial D(h_r(t))}{\partial T_r} \\ &= \frac{k\cdot 20}{\ln 10}\cdot\frac{|1+\tau_g(t)|\cdot e^{j(\angle T_r)}}{|T_r|\cdot|1+\tau_g(t)|\cdot e^{j(\angle T_r)}}, \end{aligned} \tag{8}$$

$$\begin{aligned} S_p &\triangleq \frac{\partial D(h_p(t))}{\partial T_r} \\ &= \frac{k\cdot 20}{2\cdot\ln 10}\cdot\frac{|1+\tau_g(t)|\cdot e^{j(\angle T_r)}}{|T_r|\cdot|1+\tau_g(t)|\cdot e^{j(\angle T_r)} + M\cdot e^{j(\pi+\phi_{ps})}}. \end{aligned} \tag{9}$$

In this work, the sensitivity enhancement is defined as the ratio of the sensitivity of the proposed system to that of the conventional resonator, and it can be expressed based on (8) and (9) as follows:

$$\frac{S_p}{S_r} = \frac{1}{2}\cdot\frac{|T_r|\cdot|1+\tau_g(t)|\cdot e^{j(\angle T_r)}}{|T_r|\cdot|1+\tau_g(t)|\cdot e^{j(\angle T_r)} + M\cdot e^{j(\pi+\phi_{ps})}}. \tag{10}$$

In the above equation, $\tau_g(t)$ is the unknown value to be detected, $|T_r| \gg |\tau_g(t)|$, and $|\tau_g(t)| \ll 1$. Therefore, the following conditions are necessary for effective sensitivity enhancement:

$$\begin{aligned} M &= |T_r| \\ \phi_{ps} &= \angle T_r. \end{aligned} \tag{11}$$

Thus, accurate modeling of the resonance characteristics utilizing a variable attenuator and a variable phase shifter is a key factor in improving the sensitivity. To verify the conditions shown in (11) for the effective sensitivity enhancement, the mismatch effects in magnitude and phase are analyzed. To simplify the analysis, the glucose concentration is assumed to not vary over time, i.e., $\tau_g(t) = 0$. Then, the output voltage of the RF power detector in the last stage of the proposed sensitivity enhancement system is expressed as follows:

$$\begin{aligned} &V_{out} \\ &= k\cdot 20\cdot\log_{10}\left(\frac{1}{2}\left(|T_r|\cdot e^{j(\angle T_r)} + M\cdot e^{j(\pi+\phi_{ps})}\right)\right) + V_c, \end{aligned} \tag{12}$$

and the slope of the RF power detector output is derived as follows:

$$\frac{\partial V_{out}}{\partial T_r} = \frac{k\cdot 20}{2}\cdot\ln 10\cdot\frac{e^{j(\angle T_r)}}{|T_r|\cdot e^{j(\angle T_r)} + M\cdot e^{j(\pi+\phi_{ps})}}. \tag{13}$$

When the magnitude and phase conditions derived in (11) are satisfied, the denominator of (13) becomes zero, and the slope of the RF power detector output becomes infinite. In the case of $\phi_{ps} = \angle T_r$, the effect of magnitude mismatch is shown in Fig. 2(a), while in the case of $M = |T_r|$, the effect of phase mismatch is shown in Fig. 2(b). In these figures, the maximum sensitivity enhancement can clearly be obtained when the magnitude and phase conditions are simultaneously satisfied. The magnitude condition is also demonstrated to be a more dominant factor than the phase condition in the sensitivity enhancement.

## III. Sensor Design

### A. Design of the Microwave Resonator

Microwave resonators are easy to fabricate, cost effective, and portable and have the potential for real-time detection. Because of these advantages, microwave resonators are utilized as numerous sensing devices, including for temperature [44], complex permittivity [45], vital sign [46], relative humidity [47], and breast tumor [48] sensing. Among various microwave resonators, a complementary split ring resonator (CSRR), which has a structure in which the ground plane of the microstrip transmission line is etched in the form of a double split ring, is widely used for material characterization because of its high sensitivity [49], [50].

The double split ring and an equivalent circuit of the designed rectangular CSRR are shown in Fig. 3(a). The yellow area is a ground plane made of gold-coated copper, and the gray area is a substrate. The substrate is Taconic TLY-5 A, which has a thickness of 0.762 mm, a dielectric constant of 2.17, and a tangent loss of 0.0009. The primary resonance of the CSRR occurs at the frequency where the energies of the inductance and capacitance of the CSRR are equal, and the resonant frequency is given as follows [51]:

$$f_r = \frac{1}{2\pi\sqrt{L_r(C_c + C_r)}}, \tag{14}$$

where $C_c$ is the capacitance between the signal line and the ground plane of the CSRR, and $L_r$ and $C_r$ represent the inductance and capacitance of the double split ring, respectively, as shown in Fig. 3(a). The rectangular CSRR is designed to have a resonant frequency of 2.42 GHz because it is in the industrial-scientific-medical (ISM) band. The transmission

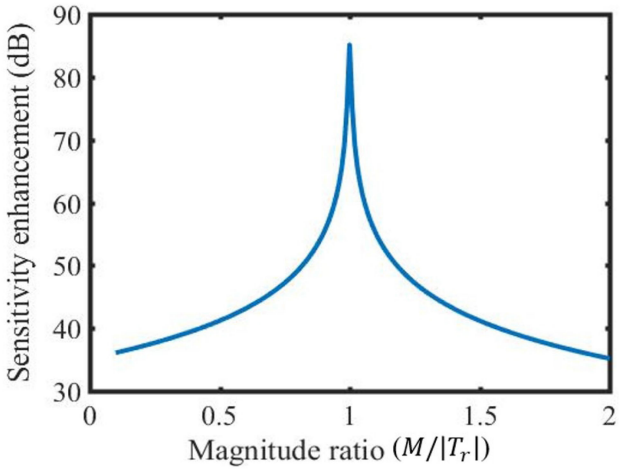


(a)

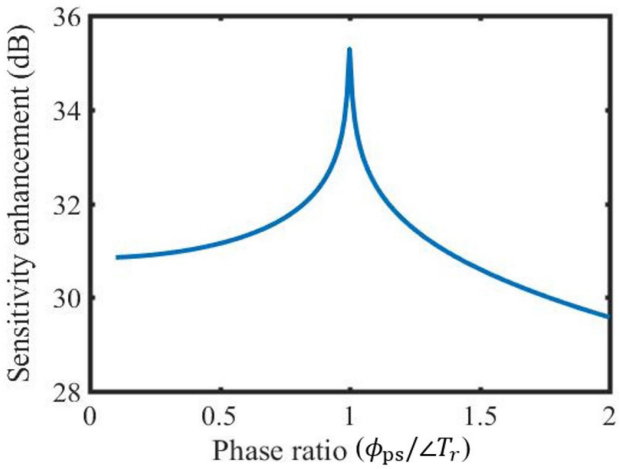


(b)

Fig. 2. Effect of mismatch conditions on sensitivity enhancement. (a) Magnitude mismatch. (b) Phase mismatch.

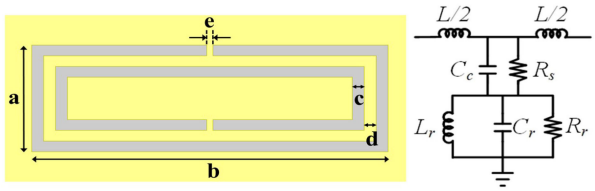


(a)

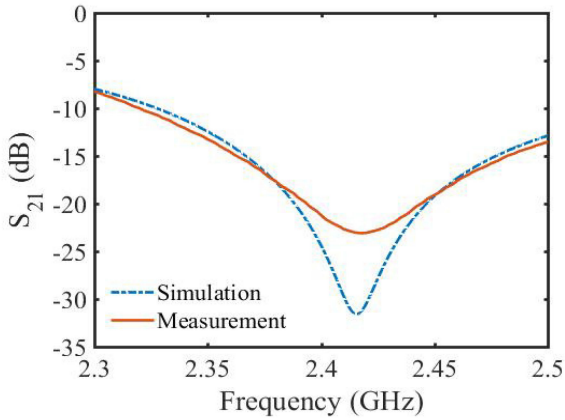


(b)

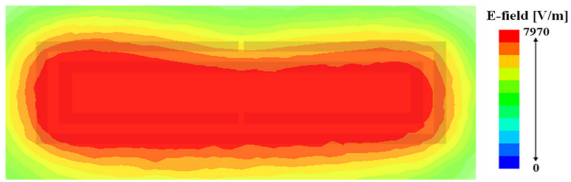


(c)

Fig. 3. Configuration and resonance characteristics of the designed rectangular CSRR. (a) Dimensions of the double split ring and equivalent circuit of the rectangular CSRR (a = 4 mm, b = 14 mm, c = 0.4 mm, d = 0.4 mm, e = 0.2 mm). (b) Comparison of transmission coefficients of the designed rectangular CSRR between the simulation and measured results. (c) Simulation result of the electric field distribution.

characteristics of the designed rectangular CSRR are simulated using a 3D full-wave electromagnetic solver (HFSS). The transmission characteristic is -31.6 dB at 2.42 GHz, as shown by the blue dotted line in Fig. 3(b). The measurement result of the designed rectangular CSRR using a VNA is shown by the orange line in Fig. 3(b). The measured transmission coefficient is -23.09 dB at 2.42 GHz. The difference in the transmission coefficient between the simulation and measurement results can be caused by fabrication losses such as soldering and structural discontinuity between the planar resonator and SMA connectors. Most microwave resonator-based sensors utilize the interaction of the near-field with the electrical properties of the material to be detected. Thus, to obtain the maximum sensitivity, the material should be placed in the area where the electric field is most strongly formed. Thus, the effective sensing area is determined to be the center of the double split ring, as clearly shown in Fig. 3(c).

### *B. Configuration of the Proposed Sensor*

Based on the schematic of the proposed sensitivity-enhanced sensor, the circuit is fabricated on a printed circuit board (Taconic TLY-5 A), as shown in Fig. 4(a) and (b). The designed rectangular CSRR, which is the main component for glucose concentration sensing, is implemented. An analog voltage-controlled variable attenuator (RFSA2033) and a variable phase shifter consisting of 2-stage varactor diodes (SMV1405) and surface mount inductors [52] are used for modeling the resonance characteristics of the rectangular CSRR. The control voltages of the variable attenuator and variable phase shifter are controlled to satisfy the magnitude and phase conditions, respectively, for the effective sensitivity enhancement. In addition, two hybrid couplers (PC2025A2700AT00) are connected to both ends of the interferometric system to obtain a 180° phase difference between the signals from the resonator and the modeling part. Finally, an RF power detector (LT5538) is connected to the end of the proposed interferometric system to measure the output voltage containing the glucose concentration information.

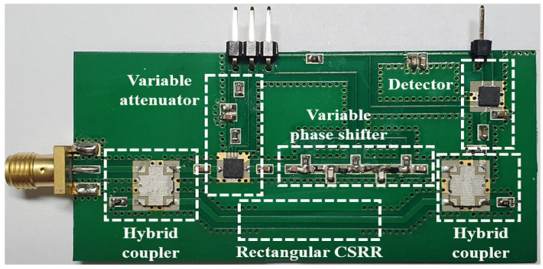


(a)

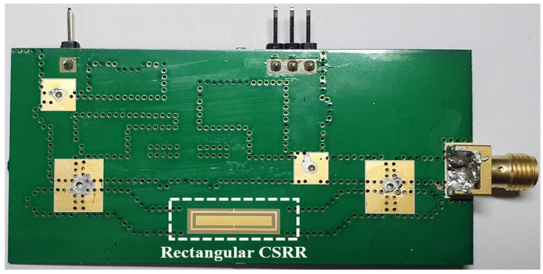


(b)

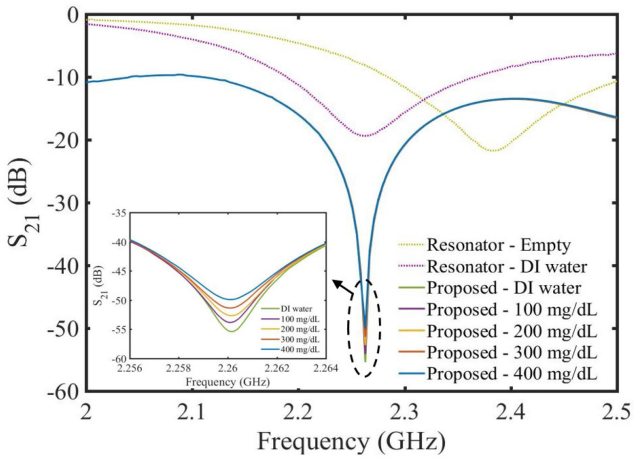


(c)

Fig. 4. Fabricated sensor. (a) Top view of the proposed sensor. (b) Bottom view of the proposed sensor. (c) Measured results of the transmission coefficient for comparison between the rectangular CSRR with an empty fluidic channel and DI water and the proposed rectangular CSRR coupled with an interferometric system with DI water and glucose solutions of 100, 200, 300, and 400 mg/dL.

An empty fluidic channel is loaded onto the surface of the center of the double split ring, which was designated as the effective sensing area in the previous subsection. The constituent of the fluidic channel is polytetrafluoroethylene (PTFE), which has a dielectric constant of 2.1, a tangent loss of 0.001, an inner diameter of 1/32 in, and an outer diameter of 1/16 in. The resonant frequency is shifted to 2.38 GHz, and the transmission coefficient of the rectangular CSRR becomes -21.75 dB due to the dielectric constant and tangent loss of the fluidic channel, as shown by the green dotted line in Fig. 4(c). When a fluidic channel containing deionized (DI) water is loaded onto the effective sensing area, the transmission coefficient of the rectangular CSRR is plotted by the violet dotted line in Fig. 4(c). The sample volume in the effective sensing area is approximately 6.9 $\mu$L. The resonant frequency is shifted to 2.26 GHz, and the transmission coefficient of the rectangular CSRR becomes -18.3 dB due to the high dielectric constant and loss of the DI water in the fluidic channel. To model the resonance characteristics, the control voltages of the variable attenuator and variable phase shifter are determined by measuring the magnitude and phase components of the designed rectangular CSRR loaded with a fluidic channel containing 6.9 $\mu$L DI water. The measured magnitude and phase of the transmission coefficient are -18.3 dB and 117.15°, respectively. Accordingly, the control voltages of the variable attenuator and variable phase shifter are set to 2.9 V and 3.38 V, respectively. To compare the transmission coefficient of the proposed system with that of the rectangular CSRR, junctions P and 2 in Fig. 1 are connected to a VNA. The transmission coefficient of the proposed system is measured to be -55.4 dB by applying the determined control voltages to the modeling part, as shown in Fig. 4(c). Moreover, the transmission coefficients of the proposed sensor loaded with a fluidic channel containing the glucose solutions in the range of 0-400 mg/dL are plotted as solid lines, as shown in Fig. 4(c). The inset offers an enlarged view of the area near the resonant frequency. When the glucose concentration is increased from 0 mg/dL to 400 mg/dL, the transmission coefficient is changed by approximately 5.4 dB.

## IV. Results and Discussion

To verify the sensitivity enhancement performance of the proposed glucose sensor, the variations in the transmission coefficient of the single rectangular CSRR and the proposed interferometric sensor system with changing glucose concentration are measured. Glucose solutions with different concentrations from 0 to 400 mg/dL are prepared considering the possible blood glucose range of a human body. To quantify the sensitivity of the rectangular CSRR, a parameter is defined as follows:

$$\Delta S_{21} = S_{21,measured} - S_{21,DIwater}(dB), \qquad (15)$$

where $S_{21,measured}$ and $S_{21,DIwater}$ are the transmission coefficients when each concentration of glucose solution and DI water flow in the fluidic channel. To measure the transmission coefficient at the resonant frequency, both ends of the rectangular CSRR are connected to the VNA. The measured results show that the variation in the transmission coefficient is 0.104 dB when the glucose concentration increases from 0 to 400 mg/dL, as shown in Fig. 5. For comparison with the sensitivity of the proposed sensor, the variation in the transmission coefficient is measured through an identical measurement procedure. Junctions P and 2 in Fig. 1 are connected to the VNA instead of the RF source and RF power detector. The measured transmission coefficient variation is 5.374 dB when increasing the glucose concentration from 0 to 400 mg/dL, as shown in Fig. 5.

To demonstrate the mismatch effects in the magnitude and phase conditions through measurement, the transmission coefficient of the proposed sensor is measured when the magnitude ratio ($M/|T_r|$) and phase ratio ($\phi_{ps}/\angle T_r$) are in the range of 0.5 to 1.5, respectively. When the magnitude and phase conditions are satisfied ($M = |T_r|$ and $\phi_{ps} = \angle T_r$), the variation in the

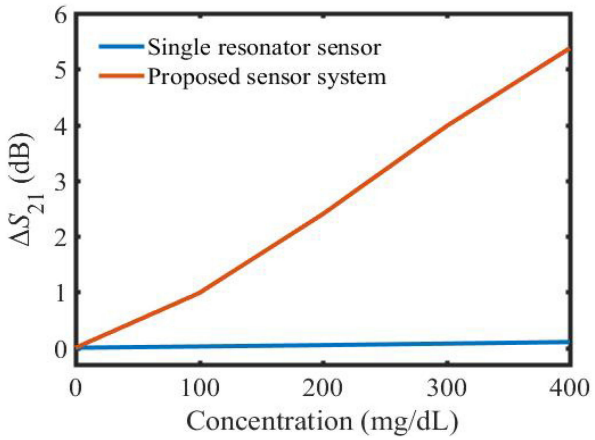


Fig. 5. Comparison of variations in the transmission coefficient with glucose concentration of the rectangular CSRR and the proposed rectangular CSRR coupled with the interferometric system.

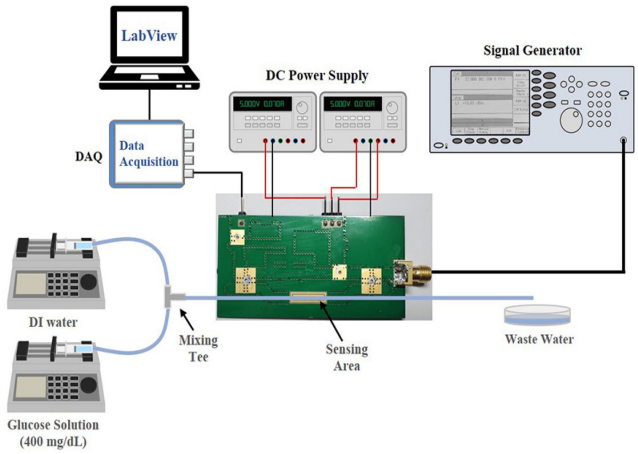


Fig. 7. Experimental setup for noninvasive and continuous glucose concentration detection.

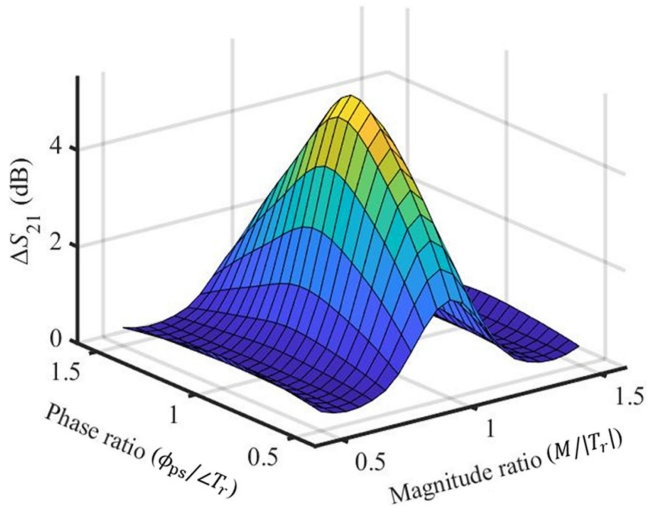


Fig. 6. Variation in the transmission coefficient according to the degree of magnitude and phase conditions satisfaction for effective sensitivity enhancement.

transmission coefficient is highest, as shown in Fig. 6. Additionally, the sensitivity is decreased with a steeper slope in the magnitude ratio direction. Thus, it is proven that the magnitude condition has more influence on the sensitivity enhancement than the phase condition. These results are in good agreement with the mathematical analysis in Section II.

As a next step, noninvasive and continuous glucose concentration detection is conducted by using two syringe pumps and a fluidic channel, as illustrated in Fig. 7. The two syringe pumps are prepared with DI water and 400 mg/dL glucose solution to implement continuous concentration control, and the glucose solution is mixed with the DI water in the mixing tee. The glucose concentration is increased gradually every 2 minutes by controlling the flow rates of the two syringe pumps, while the flow rate of the outlet is kept at 200 $\mu$L/min. The fluidic channel filled with the glucose solution is located at the center of the rectangular CSRR. A +5 V supply voltage ($V_{DD}$) and the control

TABLE I
MEAN VALUES OF THE VARIATION IN THE TRANSMISSION COEFFICIENT

| Glucose concentration (mg/dL) | Variation in output voltage (mV) |
|---|---|
| 0 | 2.4 |
| 100 | 39.2 |
| 200 | 82.8 |
| 300 | 127.9 |
| 400 | 171.6 |

voltages of the variable attenuator and phase shifter are applied by using two DC power supplies. The RF signal is generated from a signal generator (MG3695 A). The output voltage of the RF power detector is collected and stored every second by a data acquisition (DAQ) board and LabView. The temperature and relative humidity of the measurement environment are kept almost constant at $23\,^{\circ}\mathrm{C} \pm 1\,^{\circ}\mathrm{C}$ and $40\% \pm 3\%$, respectively.

The measured results are shown in Fig. 8. As the glucose concentration is varied from 0 to 400 mg/dL, the output voltage of the RF power detector is increased. When the RF power detector is connected to the rectangular CSRR, the variation in the detector output voltage is approximately 3.6 mV, as shown in Fig. 8(a). Meanwhile, when the proposed rectangular CSRR with the interferometric system is utilized, the variation in the detector output voltage is approximately 171.6 mV, as shown in Fig. 8(b), revealing 48 times sensitivity improvement. The mean values of the variation in the detector output voltage for each concentration are summarized in Table I. Based on the mean values, the glucose concentration can be predicted from the variation in detector output voltage as follows:

$$C = 2.338 \cdot \Delta V + 1.754, \tag{16}$$

where $C$ is the predicted glucose concentration in mg/dL, and $\Delta V$ is the variation in detector output in mV.

To evaluate the reliability of the proposed glucose sensor, the predicted glucose concentrations obtained from 20 repeated measurements using the relation shown in (16) are plotted in

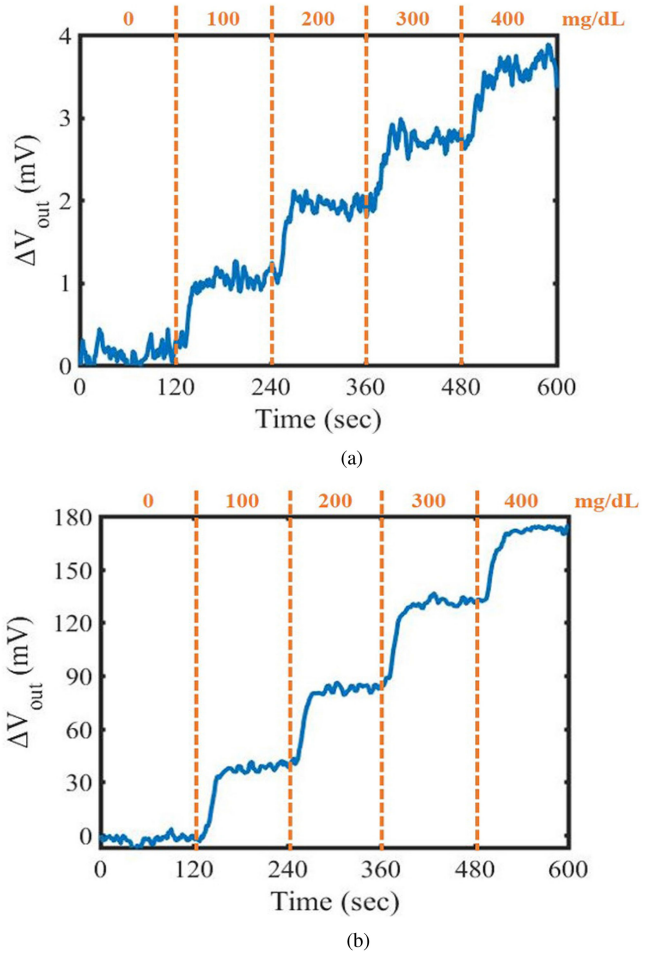


Fig. 8. Measured results of the variation in the output voltage of the RF power detector with glucose concentration. (a) Measured result of the rectangular CSRR. (b) Measured result of the proposed rectangular CSRR coupled with the interferometric system.

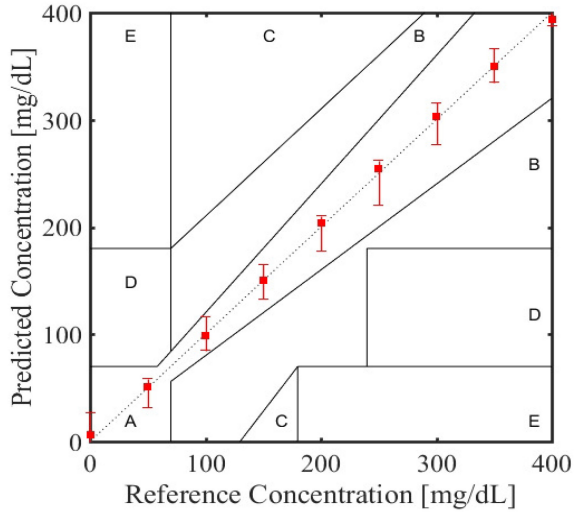


Fig. 9. Clarke error grid obtained by measuring the glucose concentration for different concentrations.

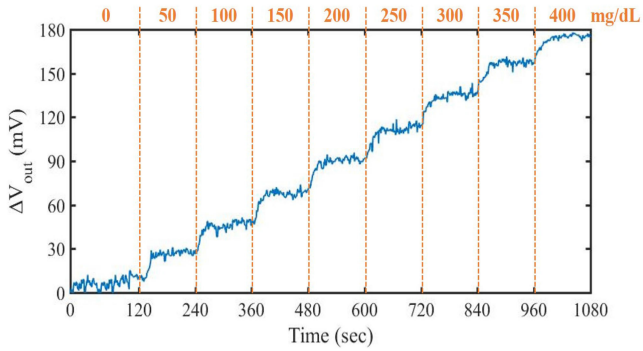


Fig. 10. Continuous measurement of the variation in the output voltage of the RF power detector when the glucose concentration is increased from 0 to 400 mg/dL with a step of 50 md/dL.

Fig. 9. The Clarke error grid is used to assess the clinical accuracy of the glucose meter [53]. The X- and Y-axes represent the real and predicted glucose concentrations, respectively. Data on the dotted diagonal line indicate perfect clinical accuracy, while data above and below the dotted diagonal line imply overestimation and underestimation, respectively. The Clarke error grid is divided into 5 zones, namely, Zones A, B, C, D, and E. Zone A is the region in which the error in the predicted glucose concentration is below 20%, and data in Zone A can be used for clinical purposes. Zone B is the region with an error of more than 20% that is considered clinically uncritical. However, Zones C, D, and E lead to dangerous failure to detect hyperglycemia and hypoglycemia. Fig. 9 shows that all the measured data closely follow the dotted diagonal line and are in Zone A. The maximum repeatability error is 17.82%. The proposed interferometric glucose sensor is demonstrated to be able to detect a critical status, such as hyperglycemia and hypoglycemia, and lead to correct clinical decisions.

Furthermore, the glucose concentration is changed from 0 to 400 mg/dL with a step of 50 mg/dL in the proposed sensitivity enhancement system to verify the limit of detection (LOD). The variation in the detector output voltage is 173.5 mV, as shown in Fig. 10, which is consistent with the previous data (Fig. 8(b)).

Moreover, since the sensitivity is increased by increasing the sample volume [59], the sensitivity in this paper is redefined as the variation in the transmission coefficient that can be obtained per unit glucose concentration and sample volume for fair comparison as follows:

$$S = \Delta S_{21} \; / \; (\Delta C_g \cdot v_g), \tag{17}$$

where $\Delta S_{21}$ is the variation in the transmission coefficient on the dB scale, $\Delta C_g$ is the change in the glucose concentration in mg/dL, and $v_g$ is the volume of the glucose solution in $\mu$L. The output voltage as a function of the input power of the RF power detector used in this study is 31.8 mV/dBm. Therefore, the sensitivity of the proposed glucose sensor on the dB scale and mV scale is as follows:

$$\begin{aligned} S_{proposed} &= 1.947 \;\; mdB/mgdL^{-1}\mu L, \\ &= 61.9 \;\; \mu V/mgdL^{-1}\mu L. \end{aligned} \tag{18}$$

TABLE II
COMPARISON OF GLUCOSE SENSOR PERFORMANCES

| Reference | Sensor Type | Frequency (GHz) | Glucose Range (mg/dL) | Lowest Concentration Measured (mg/dL) | Sample Volume ($\mu$L) | Sensing Parameter | Sensitivity (per mgdL$^{-1}\mu$L) |
|---|---|---|---|---|---|---|---|
| [54] | Chipless tag SRR | 4 | 0-720 | 90 | 200 | frequency | 10.6 Hz |
| [38] | Loss-compensated SRR | 1.156 | 0-18000 | 18 | 10 | frequency | 7.6 Hz |
| [41] | 7th IMP of an active SRR | 4 | 0-600 | 90 | 40 | frequency | 5.56 Hz |
| [55] | DSRR | 4.05 | 5-80 | 5 | 120 | $S_{21}$ level | 0.008 mdB |
| [56] | Hilbert-shaped resonator | 6 | 0-250 | 50 | 500 | $S_{21}$ level | 0.031 mdB |
| [57] | SRR | 5.16 | 0-10000 | 1000 | 25 | $S_{21}$ level | 0.003 mdB |
| [27] | CSRR | 2.42 | 0-400 | 100 | 3.9 | $S_{21}$ level | 0.019 mdB |
| [28] | CSRR | 2.42 | 0-400 | 100 | 3.9 | $S_{21}$ level | 0.021 mdB |
| [58] | LC resonator | 3.41 | 4000-20000 | 4000 | 20 | $S_{21}$ level | 0.027 mdB |
| This work | CSRR+Interferomectric system | 2.26 | 0-400 | 50 | 6.9 | $S_{21}$ level | 1.947 mdB |

To demonstrate the superior sensitivity of the proposed glucose sensor, comparisons with recently published microwave-based glucose sensors using transmission coefficient and frequency as a sensing parameter are summarized in Table II. The comparison factors are the sensor type, frequency, detected glucose concentration range, lowest glucose concentration measured, sample volume, sensing parameter, and sensitivity. The proposed glucose sensor clearly achieves outstanding sensitivity performance with a small sample volume.

## V. CONCLUSION

In this paper, a novel scheme for a sensitivity-enhanced glucose sensor based on a microwave resonator and an interferometric system is proposed for noninvasive continuous glucose concentration detection. The proposed sensor consists of a rectangular CSRR for glucose concentration detection, a variable attenuator and a variable phase shifter to model the resonance characteristics of the microwave resonator, two hybrid couplers to obtain a $180^\circ$ phase difference, and an RF power detector for convenient and continuous measurement. The fluidic system with two syringe pumps allows noninvasive continuous glucose detection. To improve the sensitivity of the sensor, the proposed system is mathematically analyzed, and both the magnitude and phase conditions for the effective sensitivity enhancement are derived.

The performance of the proposed glucose sensor is verified by comparing the measurement results obtained with the single rectangular CSRR and the proposed interferometric system. The variations in the transmission coefficient for the single rectangular CSRR and the proposed interferometric system with increasing glucose concentration from 0 to 400 mg/dL are 0.104 dB and 5.374 dB, respectively. Moreover, the continuous measurement results of the detector output voltage show that the proposed glucose sensor has a sensitivity 48 times that of the rectangular CSRR, indicating a dramatic improvement in the sensitivity. The proposed glucose sensor is clearly demonstrated to have superior performance compared with other microwave resonator-based glucose sensors. Discrimination of the effect of glucose from that of other components in human blood could be a future work. Furthermore, in vivo testing of the advanced glucose sensor will be performed.

## REFERENCES


[1] P. Saeedi *et al.*, "Global and regional diabetes prevalence estimates for 2019 and projections for 2030 and 2045: Results from the international diabetes federation diabetes atlas, *9th edition*," *Diabetes Res. Clin. Pract.*, vol. 157, 2019, Art. no. 107843.

[2] P. Saeedi *et al.*, "Mortality attributable to diabetes in 20-79 years old adults, 2019 estimates: Results from the international diabetes federation diabetes atlas, 9th edition," *Diabetes Res. Clin. Pract.*, vol. 162, 2020, Art. no. 108086.

[3] C. H. Wei and S. E. Litwin, "Hyperglycemia and adverse outcomes in acute coronary syndromes: Is serum glucose the provocateur or innocent bystander?" *Diabetes*, vol. 63, no. 7, pp. 2209–2212, 2014.

[4] G. E. Umpierrez and F. J. Pasquel, "Management of inpatient hyperglycemia and diabetes in older adults," *Diabetes Care*, vol. 40, no. 4, pp. 509–517, 2017.

[5] K. V. Narayan and U. P. Gujral, "Evidence tips the scale toward screening for hyperglycemia," *Diabetes Care*, vol. 38, no. 8, pp. 1399–1401, 2015.

[6] A. D. A. W. on Hypoglycemia, "Defining and reporting hypoglycemia in diabetes," *Diabetes Care*, vol. 28, no. 5, pp. 1245–1249, 2005.

[7] S.-W. Yi, S. Park, Y.-H. Lee, B. Balkau, and J.-J. Yi, "Fasting glucose and all-cause mortality by age in diabetes: A prospective cohort study," *Diabetes Care*, vol. 41, no. 3, pp. 623–626, 2018.

[8] R. Williams *et al.*, "Global and regional estimates and projections of diabetes-related health expenditure: Results from the international diabetes federation diabetes atlas, 9th edition," *Diabetes Res. Clin. Pract.*, vol. 162, 2020, Art. no. 108072.

[9] S. Sharma, Z. Huang, M. Rogers, M. Boutelle, and A. E. G. Cass, "Evaluation of a minimally invasive glucose biosensor for continuous tissue monitoring," *Anal. Bioanal. Chem.*, vol. 408, no. 29, pp. 8427–8435, 2016.

[10] M. Wu *et al.*, "Assisted 3D printing of microneedle patches for minimally invasive glucose control in diabetes," *Mater. Sci. Eng. C*, vol. 117, 2020, Art. no. 111299.

[11] P. Bollella, S. Sharma, A. E. G. Cass, F. Tasca, and R. Antiochia, "Minimally invasive glucose monitoring using a highly porous gold microneedles-based biosensor: Characterization and application in artificial interstitial fluid," *Catalysts*, vol. 9, no. 7, p. 580, 2019.

[12] E. Topsakal, T. Karacolak, and E. C. Moreland, "Glucose-dependent dielectric properties of blood plasma," in *Proc. 30th URSI Gen. Assem. Sci. Symp.*, Aug. 2011, pp. 1–4.

[13] S. Saha *et al.*, "A glucose sensing system based on transmission measurements at millimetre waves using micro strip patch antennas," *Sci. Rep.*, vol. 7, 2017, Art. no. 6855.

[14] B. Camli, E. Kusakci, B. Lafci, S. Salman, H. Torun, and A. Yalcinkaya, "A microwave ring resonator based glucose sensor," *Procedia Eng.*, vol. 168, pp. 465–468, 2016.

[15] S. Zeising *et al.*, "Towards realisation of a non-invasive blood glucose sensor using microstripline," in *Proc. IEEE Int. Instrum. Meas. Technol. Conf.*, May 2020, pp. 1–6.

[16] B. Camli, E. Kusakci, B. Lafci, S. Salman, H. Torun, and A. D. Yalcinkaya, "Cost-effective, microstrip antenna driven ring resonator microwave biosensor for biospecific detection of glucose," *IEEE J. Sel. Top. Quantum Electron.*, vol. 23, no. 2, pp. 404–409, Mar./Apr. 2017.

[17] G.-H. Yun, "A study on slot coupled capacitor resonator for non-invasive glucose monitoring in earlobe," *J. Korea Inst. Electromagn. Eng. Sci.*, vol. 28, no. 4, pp. 279–285, 2017.

[18] K. Lee, A. Babajanyan, C. Kim, S. Kim, and B. Friedman, "Glucose aqueous solution sensing by a near-field microwave microprobe," *Sens. Actuators A. Phys.*, vol. 148, no. 1, pp. 28–32, 2008.

[19] S. Kiani, P. Rezaei, M. Karami, and R. A. Sadeghzadeh, "Band-stop filter sensor based on SIW cavity for the non-invasive measuring of blood glucose," *IET Wireless Sens. Syst.*, vol. 9, no. 1, pp. 1–5, 2019.

[20] S. Kim *et al.*, "Noninvasive in vitro measurement of pig-blood d-glucose by using a microwave cavity sensor," *Diabetes Res. Clin. Pract.*, vol. 96, no. 3, pp. 379–384, 2012.

[21] A. Bababjanyan, H. Melikyan, S. Kim, J. Kim, K. Lee, and B. Friedman, "Real-time noninvasive measurement of glucose concentration using a microwave biosensor," *J. Sens.*, vol. 2010, 2010, Art. no. 452163.

[22] Y. Fan, X. Deng, Q. Wang, and W. Wang, "Testing glucose concentration in aqueous solution based on microwave cavity perturbation technique," in *Proc. 3rd Int. Conf. Biomed. Eng. Inform.*, Oct. 2010, pp. 1046–1049.

[23] A. A. M. Bahar, Z. Zakaria, M. K. M. Arshad, A. A. M. Isa, Y. Dasril, and R. A. Alahnomi, "Real time microwave biochemical sensor based on circular SIW approach for aqueous dielectric detection," *Sci. Rep.*, vol. 9, no. 1, 2019, Art. no. 5467.

[24] G. Govind and M. J. Akhtar, "Metamaterial-inspired microwave microfluidic sensor for glucose monitoring in aqueous solutions," *IEEE Sens. J.*, vol. 19, no. 24, pp. 11 900–11 907, Dec. 2019.

[25] A. E. Omer *et al.*, "Low-cost portable microwave sensor for non-invasive monitoring of blood glucose level: Novel design utilizing a four-cell CSRR hexagonal configuration," *Sci. Rep.*, vol. 10, no. 1, 2020, Art. no. 15200.

[26] V. Turgul and I. Kale, "Permittivity extraction of glucose solutions through artificial neural networks and non-invasive microwave glucose sensing," *Sens. Actuators A Phys.*, vol. 277, pp. 65–72, 2018.

[27] C. Jang, J.-K. Park, H.-J. Lee, G.-H. Yun, and J.-G. Yook, "Temperature-corrected fluidic glucose sensor based on microwave resonator," *Sensors*, vol. 18, no. 11, 2018, Art. no. 3850.

[28] C. Jang, J. Park, H. Lee, G. Yun, and J. Yook, "Non-invasive fluidic glucose detection based on dual microwave complementary split ring resonators with a switching circuit for environmental effect elimination," *IEEE Sens. J.*, vol. 20, no. 15, pp. 8520–8527, Aug. 2020.

[29] A. Ebrahimi, J. Scott, and K. Ghorbani, "Microwave reflective biosensor for glucose level detection in aqueous solutions," *Sens. Actuators A Phys.*, vol. 301, 2020, Art. no. 111662.

[30] R. Kumari, P. N. Patel, and R. Yadav, "An ENG resonator-based microwave sensor for the characterization of aqueous glucose," *J. Phys. D: Appl. Phys.*, vol. 51, no. 7, 2018, Art. no. 075601.

[31] N. Kim, R. Dhakal, K. Adhikari, E. Kim, and C. Wang, "A reusable robust radio frequency biosensor using microwave resonator by integrated passive device technology for quantitative detection of glucose level," *Biosensors Bioelectron.*, vol. 67, pp. 687–693, 2015.

[32] A. Ebrahimi, W. Withayachumnankul, S. F. Al-Sarawi, and D. Abbott, "Microwave microfluidic sensor for determination of glucose concentration in water," in *Proc. IEEE 15th Mediterranean Microw. Symp.*, Dec. 2015, pp. 1–3.

[33] C. Jang, J.-K. Park, G.-H. Yun, and J.-G. Yook, "Noninvasive method to distinguish between glucose and sodium chloride solution using complementary split-ring resonator," *J. Korea Inst. Electromagn. Eng. Sci.*, vol. 29, no. 4, pp. 247–255, 2018.

[34] H. Choi *et al.*, "Design and in vitro interference test of microwave non-invasive blood glucose monitoring sensor," *IEEE Trans. Microw. Theory Techn.*, vol. 63, no. 10, pp. 3016–3025, Oct. 2015.

[35] M. Abdolrazzaghi and M. Daneshmand, "Sensitivity optimization in SRRS using interferometry phase cancellation," in *Proc. IEEE MTT-S Int. Microw. Symp.*, May 2019, pp. 1495–1498.

[36] M. C. Jain, A. V. Nadaraja, S. Mohammadi, B. M. Vizcaino, and M. H. Zarifi, "Passive microwave biosensor for real-time monitoring of subsurface bacterial growth," *IEEE Trans. Biomed. Circuits Syst.*, vol. 15, no. 1, pp. 122–132, Feb. 2021.

[37] M. Abdolrazzaghi, M. Daneshmand, and A. K. Iyer, "Strongly enhanced sensitivity in planar microwave sensors based on metamaterial coupling," *IEEE Trans. Microw. Theory Tech.*, vol. 66, no. 4, pp. 1843–1855, Apr. 2018.

[38] M. Abdolrazzaghi, N. Katchinskiy, A. Elezzabi, P. E. Light, and M. Daneshmand, "Noninvasive glucose sensing in aqueous solutions using an active split-ring resonator," *IEEE Sens. J.*, vol. 21, no. 17, pp. 18742–18755, Sep. 2021.

[39] M. H. Zarifi, S. Farsinezhad, K. Shankar, and M. Daneshmand, "Liquid sensing using active feedback assisted planar microwave resonator," *IEEE Microw. Wireless Compon. Lett.*, vol. 25, no. 9, pp. 621–623, Sep. 2015.

[40] M. H. Zarifi and M. Daneshmand, "Non-contact liquid sensing using high resolution microwave microstrip resonator," in *Proc. IEEE MTT-S Int. Microw. Symp.*, Jul. 2015, pp. 1–4.

[41] M. Abdolrazzaghi and M. Daneshmand, "Exploiting sensitivity enhancement in micro-wave planar sensors using intermodulation products with phase noise analysis," *IEEE Trans. Circuits Syst. I Regular Papers*, vol. 67, no. 12, pp. 4382–4395, Dec. 2020.

[42] Y.-J. An, G.-H. Yun, and J.-G. Yook, "Sensitivity enhanced vital sign detection based on antenna reflection coefficient variation," *IEEE Trans. Biomed. Circuits Syst.*, vol. 10, no. 2, pp. 319–327, Apr. 2016.

[43] B.-H. Kim, Y.-J. An, G.-H. Yun, and J.-G. Yook, "Rf interferometric wearable wrist pulse detection system," *IET Microw. Antennas Propag.*, vol. 12, no. 2, pp. 167–172, 2018.

[44] J. Xiong *et al.*, "Dielectrically-loaded cylindrical resonator-based wireless passive high-temperature sensor," *Sensors*, vol. 16, 2016, Art. no. 2037.

[45] A. Ebrahimi, J. Scott, and K. Ghorbani, "Ultrahigh-sensitivity microwave sensor for microfluidic complex permittivity measurement," *IEEE Trans. Microw. Theory Techn.*, vol. 67, no. 10, pp. 4269–4277, Oct. 2019.

[46] J. K. Park *et al.*, "Noncontact RF vital sign sensor for continuous monitoring of driver status," *IEEE Trans. Biomed. Circuits Syst.*, vol. 13, no. 3, pp. 493–502, Jun. 2019.

[47] J. K. Park, C. Jang, G. H. Yun, H. J. Lee, H. H. Choi, and J. G. Yook, "Sensitive relative humidity monitoring sensor based on microwave active resonator with PEDOT:PSS," *IEEE Access*, vol. 8, pp. 166 283–166 293, Sep. 2020.

[48] S. M. Aguilar, M. A. Al-Joumayly, M. J. Burfeindt, N. Behdad, and S. C. Hagness, "Multiband miniaturized patch antennas for a compact, shielded microwave breast imaging array," *IEEE Trans. Antennas Propag.*, vol. 62, no. 3, pp. 1221–1231, Mar. 2014.

[49] M. A. H. Ansari, A. K. Jha, and M. J. Akhtar, "Design and application of the CSRR-based planar sensor for noninvasive measurement of complex permittivity," *IEEE Sensors J.*, vol. 15, no. 12, pp. 7181–7189, Dec. 2015.

[50] A. Ebrahimi, W. Withayachumnankul, S. Al-Sarawi, and D. Abbott, "High-sensitivity metamaterial-inspired sensor for microfluidic dielectric characterization," *IEEE Sensors J.*, vol. 14, no. 5, pp. 1345–1351, May 2014.

[51] M. S. Boybay and O. M. Ramahi, "Material characterization using complementary split-ring resonators," *IEEE Trans. Instrum. Meas.*, vol. 61, no. 11, pp. 3039–3046, Nov. 2012.

[52] H. Kim, A. B. Kozyrev, A. Karbassi, and D. W. van der Weide, "Linear tunable phase shifter using a left-handed transmission line," *IEEE Microw. Wireless Compon. Lett.*, vol. 15, no. 5, pp. 366–368, May 2005.

[53] W. L. Clarke, D. Cox, L. A. Gonder-Frederick, W. Carter, and S. L. Pohl, "Evaluating clinical accuracy of systems for self-monitoring of blood glucose," *Diabetes Care*, vol. 10, no. 5, pp. 622–628, 1987.

[54] M. Baghelani, Z. Abbasi, M. Daneshmand, and P. E. Light, "Non-invasive continuous-time glucose monitoring system using a chipless printable sensor based on split ring microwave resonators," *Sci. Rep.*, vol. 10, no. 1, 2020, Art. no. 12980.

[55] S. Mohammadi, A. V. Nadaraja, D. J. Roberts, and M. H. Zarifi, "Real-time and hazard-free water quality monitoring based on microwave planar resonator sensor," *Sens. Actuators A Phys.*, vol. 303, 2020, Art. no. 111663.

[56] L. Odabashyan *et al.*, "Real-time noninvasive measurement of glucose concentration using a modified hilbert shaped microwave sensor," *Sensors*, vol. 19, no. 24, 2019, Art. no. 5525.

[57] C. G. Juan, E. Bronchalo, B. Potelon, C. Quendo, E. Ávila-Navarro, and J. M. Sabater-Navarro, "Concentration measurement of microliter-volume water-glucose solutions using $Q$ factor of microwave sensors," *IEEE Trans. Instrum. Meas.*, vol. 68, no. 7, pp. 2621–2634, Jul. 2019.

[58] S. Harnsoongnoen and A. Wanthong, "Coplanar waveguide transmission line loaded with electric-LC resonator for determination of glucose concentration sensing," *IEEE Sensors J.*, vol. 17, no. 6, pp. 1635–1640, Mar. 2017.

[59] J. Kim, A. Babajanyan, A. Hovsepyan, K. Lee, and B. Friedman, "Microwave dielectric resonator biosensor for aqueous glucose solution," *Rev. Sci. Instrum.*, vol. 79, no. 8, 2008, Art. no. 0 86107.

**Chorom Jang** (Graduate Student Member, IEEE) was born in Incheon, South Korea. She received the B.S. degree in electronic engineering from Seokyeong University, Seoul, South Korea, in 2017. She is currently working toward the Ph.D. degree in electrical and electronics engineering with Yonsei University, Seoul. Her main research interests include RF-based sensors, such as glucose, vital signs, pressure sensors, and microwave components/systems.

**Jin-Kwan Park** (Graduate Student Member, IEEE) was born in Seoul, South Korea. He received the B.S. degree in electronics and electrical engineering from Dongguk University, Seoul, South Korea, in 2014. He is currently working toward the Ph.D. degree in electrical and electronics engineering with Yonsei University, Seoul. His main research interests include RF-based sensors, such as vital signs, humidity, glucose, and gas sensors, and microwave/millimeter-wave components/systems.

**Hee-Jo Lee** (Member, IEEE) received the Ph.D. degree in electrical and electronic engineering from Yonsei University, Seoul, South Korea, in 2010. From 2010 to 2012, he worked with the Electrical and Electronic Engineering Department, Yonsei University and the Graphene Research Institute, Sejong University, Seoul, South Korea, as a Postdoctoral Researcher. From April 2012 to August 2014, he worked with the Mechanical Engineering, and Electrical and Electronic Engineering Departments, Yonsei University, as a Research Professor. Since September 2014, he has been an Assistant Professor with the Department of Physics Education, Daegu University. His main research interests include the areas of electromagnetic wave and field theory, RF/microwave bio- and gas sensors, RF/microwave circuit modeling and characterization of carbon nanomaterials, including graphene, graphene ribbons, graphene oxide, and electromagnetic metamaterials for biosensing.

**Gi-Ho Yun** was born in Jeonju-Si, South Korea. He received the M.S. and Ph.D. degrees in electronics engineering from Yonsei University, Seoul, South Korea, in 1986 and 1999, respectively. From 1985 to 1997, he was with Samsung Electronics and Samsung Electro-Mechanics. Then, he was with Honam University, Gwangju, South Korea, from 1997 to 2008. He is currently a Professor with the Division of Information and Communication Engineering, Sungkyul University, Anyang, South Korea. He is also with the Advanced Computational Electromagnetic Laboratory, Yonsei University. His current research interests include the areas of active and passive circuitry at RF/MW frequencies and various sensors to detect vital signs and biosignals in the human body.

**Jong-Gwan Yook** (Senior Member, IEEE) was born in Seoul, South Korea. He received the B.S. and M.S. degrees in electronics engineering from Yonsei University, Seoul, South Korea, and the Ph.D. degree from the University of Michigan, Ann Arbor, MI, USA, in 1987, 1989, and 1996, respectively. He is currently a Professor with the School of Electrical and Electronic Engineering, Yonsei University. His main research interests include the areas of theoretical/numerical electromagnetic modeling and characterization of microwave/millimeter-wave circuits and components, design of radio frequency integrated circuits (RFICs) and monolithic microwave integrated-circuits (MMICs), and analysis and optimization of high-frequency high-speed interconnects, including the signal/power integrity (EMI/EMC), based on frequency- and time-domain full-wave methods. Currently, his research team developed various biosensors, such as carbon nanotube RF biosensors, for nanometer-size antigen-antibody detection and remote wireless vital sign monitoring sensors.